Two Synthetic Antibodies that Recognize and Neutralize Distinct Proteolytic Forms of the Ebola Virus Envelope Glycoprotein

Jayne F. Koellhoffer,[a] Gang Chen,[b] Rohini G. Sandesara,[c] Shridhar Bale,[d] Erica Ollmann Saphire,[d] Kartik Chandran,*[c] Sachdev S. Sidhu,*[b] and Jonathan R. Lai*[a]

Ebola virus (EBOV) is a highly pathogenic member of the *Filoviridae* family of viruses that causes severe hemorrhagic fever. Infection proceeds through fusion of the host cell and viral membranes, a process that is mediated by the viral envelope glycoprotein (GP). Following endosomal uptake, a key step in viral entry is the proteolytic cleavage of GP by host endosomal cysteine proteases. Cleavage exposes a binding site for the host cell receptor Niemann-Pick C1 (NPC1) and may induce conformational changes in GP leading to membrane fusion. However, the precise details of the structural changes in GP associated with proteolysis and the role of these changes in viral entry have not been established. Here, we have employed synthetic antibody technology to identify antibodies targeting EBOV GP prior to and following proteolysis (i.e. in the "uncleaved" [GP_{UNCL}] and "cleaved" [GP_{CL}] forms). We identified antibodies with distinct recognition profiles: Fab_{CL} bound preferentially to GP_{CL} ($EC_{50} = 1.7$ nM), whereas Fab_{UNCL} bound specifically to GP_{UNCL} ($EC_{50} = 75$ nM). Neutralization assays with GP-containing pseudotyped viruses indicated that these antibodies inhibited GP_{CL}- or GP_{UNCL}-mediated viral entry with specificity matching their recognition profiles (IC_{50}: 87 nM for IgG_{CL}; 1 μM for Fab_{UNCL}). Competition ELISAs indicate that Fab_{CL} binds an epitope distinct from that of KZ52, a well-characterized EBOV GP antibody, and from that of the luminal domain of NPC1. The binding epitope of Fab_{UNCL} was also distinct from that of KZ52, suggesting that Fab_{UNCL} binds a novel neutralization epitope on GP_{UNCL}. Furthermore, the neutralizing ability of Fab_{CL} suggests that there are targets on GP_{CL} available for neutralization. This work showcases the applicability of synthetic antibody technology to the study of viral membrane fusion, and provides new tools for dissecting intermediates of EBOV entry.

Introduction

Ebola virus is a member of the family *Filoviridae* of negative-stranded, enveloped viruses ("filoviruses") that cause severe hemorrhagic fever.[1,2] The *Zaire* species (EBOV) and two others (*Sudan* and *Bundibugyo*) have been associated with large outbreaks that have up to 90% human case fatality rates.[3,4] Despite the increasing re-emergence of EBOV and outbreaks of new species,[5,6] there are currently no treatments or vaccines approved for use in humans in the United States. As with other enveloped viruses, EBOV entry into host cells requires fusion of the viral and host cell membranes, a process that is mediated by the envelope glycoprotein (GP).[7–9] In its native ("prefusion") form, GP contains three copies each of the two subunits, GP1 (the surface subunit) and GP2 (the transmembrane subunit) (Figure 1).[10,11] GP1, the larger of the two subunits (130 kDa), is responsible for cell attachment. It also contains a heavily glycoslyated mucin-like domain (muc) that projects from its surface and may play a role in immune evasion.[11] GP2 is much smaller (24 kDa) and contains two heptad repeat regions (N-terminal and C-terminal, NHR and CHR, respectively) that form a highly stable six-helix bundle in the postfusion conformation. Folding of the six-helix bundle during viral entry provides the driving force for fusion between the viral and host cell membranes. In the prefusion conformation, GP1 is closely associated with GP2, and the two are tethered together through a disulfide bond. GP2 is anchored to the viral membrane by its transmembrane domain.[10,11] Upon viral attachment and uptake, priming and triggering events in endosomal compartments release constraints on prefusion GP, resulting in deployment of the fusion machinery.[12]

A key step in the entry process is the proteolytic cleavage of GP by host cysteine proteases present in the endosome. *Zaire* EBOV appears to be dependent on the cysteine proteases cath-

[a] J. F. Koellhoffer,[+] Prof. Dr. J. R. Lai
    Department of Biochemistry, Albert Einstein College of Medicine
    1300 Morris Park Avenue, Bronx, NY 10461 (USA)
    E-mail: jon.lai@einstein.yu.edu

[b] Dr. G. Chen,[+] Prof. Dr. S. S. Sidhu
    Banting and Best Department of Medical Research
    Terrence Donnelly Centre for Cellular and Biomolecular Research
    University of Toronto
    160 College Street, Toronto, Ontario M5S 3E1 (Canada)
    E-mail: sachdev.sidhu@utoronto.ca

[c] R. G. Sandesara,[+] Prof. Dr. K. Chandran
    Department of Microbiology and Immunology
    Albert Einstein College of Medicine
    1300 Morris Park Avenue, Bronx, NY 10461 (USA)
    E-mail: kartik.chandran@einstein.yu.edu

[d] Dr. S. Bale, Prof. Dr. E. Ollmann Saphire
    Department of Immunology and Microbial Science and
    The Skaggs Institute for Chemical Biology, The Scripps Research Institute
    10550 North Torrey Pines Road, La Jolla, CA 92037 (USA)

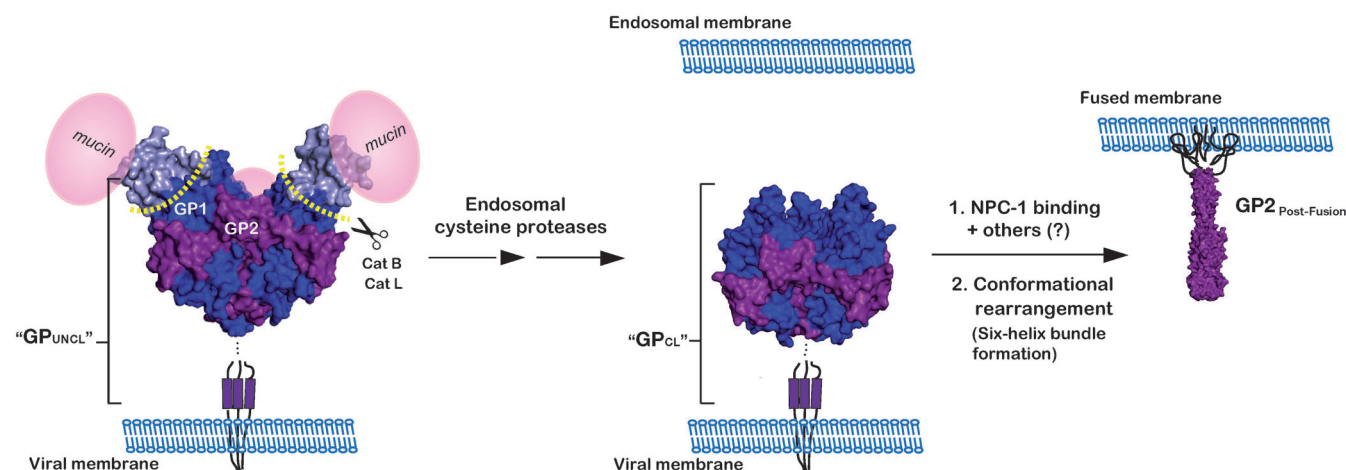[+] These authors contributed equally to this work.

WILEY ONLINE LIBRARY

These are not the final page numbers! ↗↗

Figure 1. Schematic of the EBOV glycoprotein, GP, throughout its proposed structural transitions during entry into host cells. EBOV GP contains three copies each of a 130 kDa surface subunit, GP1 (blue), and a 24 kDa transmembrane subunit, GP2 (purple). GP1 contains a heavily glycosylated carboxy-terminal mucin-like domain (represented by pink spheres, "mucin"). GP2 contains a distinct hydrophobic patch at the N terminus (the fusion peptide) and N-terminal and C-terminal heptad repeat regions (NHRs and CHRs, respectively). After the virus is taken up into the endocytic pathway, endosomal cysteine proteases cathepsins B and L (Cat B and Cat L) cleave and remove the glycan cap and mucin-like domains of GP1. In response to an unknown trigger, the cleaved GP next undergoes a large conformational change, resulting in the formation of a stable six-helix bundle. Formation of this six-helix bundle is thought to provide the energy required for fusion of the viral and host cell membranes. Here, GP is depicted in its prefusion trimer (PDB ID: 3CSY[10]) both before and after cathepsin cleavage and in its postfusion six-helix bundle (GP2$_{Post-Fusion}$; PDB ID: 1EBO[54]). The antigens used for the selection (GP$_{UNCL}$ and GP$_{CL}$) are soluble forms (i.e. lacking the transmembrane domain) of GP prior to and following proteolysis (respectively). The model for GP$_{CL}$ was generated by modifying the PDB file for GP$_{UNCL}$ (PBD ID: 3CSY) to reflect the residues that are removed during cathepsin cleavage.[43]

epsin B and cathepsin L (Cat B and Cat L) for entry;[12–14] however, other filoviruses vary in their dependence on these two proteases.[15] The proteolytic cleavage event removes most of GP1, leaving only a small 17 kDa fragment, and is necessary, but not sufficient, to trigger viral membrane fusion.[16] GP cleavage appears to play at least two roles in entry. First, cleavage is thought to unmask a binding site for the endosomal cholesterol transporter Niemann-Pick C1 (NPC1), which was recently shown to be a critical intracellular receptor for filovirus entry.[17–19] Second, proteolytic cleavage may prime GP2 for conformational change by removing constraints imposed by GP1.[12, 13, 20] In analogy to other enveloped viruses, the next step of EBOV entry involves a dramatic conformational change in the proteolytically cleaved GP, leading to projection of the GP2 N-terminal fusion loop into the host cell membrane. GP2 is then thought to collapse into the stable postfusion six-helix bundle, supplying the energy needed to overcome barriers associated with membrane fusion[7, 8] (Figure 1). Despite recent progress, many questions remain regarding EBOV viral entry. Structural changes in GP associated with endosomal proteolytic cleavage are incompletely defined, and our understanding of these changes derives from in vitro experiments; no probes are currently available to detect cleaved forms of GP generated within the endosomes of intact cells.

Monoclonal antibodies are essential reagents for understanding viral membrane fusion and identifying epitopes for immunotherapy or vaccine development. In the well-studied systems of HIV-1 and influenza, conformation- or strain-specific antibodies targeting the viral envelope glycoproteins have been used to discern which conformations are most relevant to membrane fusion and how such conformations could be mimicked by designed immunogens.[21–27] Furthermore, antibodies that have high specificity for epitopes or conformational intermediates critical to the viral membrane fusion pathway typically have high neutralization potency and, therefore, immunotherapeutic promise. B-cell repertoires from HIV-1 or influenza survivors, isolated by phage display or other methods, have been a fruitful source of neutralizing antibodies for these purposes.[28–31] However, there are limited natural sources of human EBOV antibodies targeting fusion-relevant forms of GP because survivors typically have low antibody titers, and most antibodies that arise from natural infection react preferentially with a soluble form of GP (sGP) that is secreted by the virus but is not relevant to membrane fusion.[32–34] At present, only two neutralizing antibodies targeting GP have been structurally characterized.[35–37] Other antibodies that target various epitopes of GP have been reported, but none of these harbors a human framework.

Here we describe the isolation of new GP-targeting antibodies from synthetic antibody repertoires. Synthetic antibody technology is a powerful approach toward the identification and characterization of monoclonal antibodies. Structural and bioinformatic analysis of existing antibody–antigen structures provides insight into which residues have optimal physicochemical characteristics for molecular recognition. In the most extreme case, antibody libraries in which positions in the complementarity-determining regions (CDRs) vary between only two residues—Tyr and Ser—are sufficient to support specific and high affinity antigen interactions against some targets.[38, 39] The in vitro nature of the selection process, and the fact that synthetic repertoires are predicated on principles of protein recognition rather than immune response, permits identifica-

tion of antibody fragments against targets that have resisted traditional antibody isolation methods. Furthermore, the stringency of the selections can be highly controlled, and it is therefore possible to identify antibodies with unique or enhanced specificity profiles (e.g., see refs. [40]–[42]).

Results and Discussion

Identification of synthetic antibodies that recognize distinct forms of GP

We sought to identify antibody fragments with orthogonal binding and neutralization specificities for the prefusion and proteolytically cleaved intermediate forms of EBOV GP. We employed a synthetic antigen binding fragment (Fab) library, as such libraries have demonstrated utility against nonimmunogenic targets. "Library F" contains binomial Tyr/Ser randomization in nonstructural positions of CDR-H1 and CDR-H2, and additional variation at CDR-L3 and CDR-H3 that encodes the nine residues Tyr/Ser/Gly/Ala/Phe/Trp/His/Pro/Val in a 5:4:4: 2:1:1:1: 1:1 ratio (Figure 2A). This amino acid distribution mimics the observed distribution in natural CDR segments.[38] Antibodies against over 100 diverse antigens with high affinities and specificities have been identified using Library F (Sidhu, unpublished and [57]). Full details for Library F synthesis and characteri-

zation will be published elsewhere; the diversity was 3×10^{10} unique members.

Previous work has demonstrated that the soluble form of EBOV GP lacking the transmembrane region and the mucin-like domain serves as a structural mimic for the prefusion form (GP$_{UNCL}$).[12,19] In addition, treatment of GP$_{UNCL}$ with thermolysin mimics proteolysis by Cat L and Cat B (GP$_{CL}$).[14,16,43] We therefore used soluble GP$_{UNCL}$ and GP$_{CL}$ ectodomains as surrogates for the membrane-bound prefusion and proteolytic intermediate forms, respectively, in phage display selections to isolate Fabs from Library F. After four or five rounds of selection against GP$_{UNCL}$ or GP$_{CL}$, respectively, clones displaying at least tenfold preference for GP$_{UNCL}$ or GP$_{CL}$ over a negative control protein were tested for selectivity between the two forms of GP. We identified two Fab-phage clones with unique recognition properties on-phage; surprisingly, both were isolated from selection against the GP$_{CL}$ ectodomain. These two clones exhibited the best specificity for GP$_{UNCL}$ or GP$_{CL}$ out of a panel of 12 selected clones that were characterized extensively. Fab$_{CL}$ bound preferentially to GP$_{CL}$, and Fab$_{UNCL}$ bound preferentially to GP$_{UNCL}$. Both clones displayed moderate levels of cross-reactivity for the different forms of GP, but nonetheless had distinct preferences (Figure 2B and 2C). Interestingly, both clones contain long CDR-H3 loops with a distribution of aromatic (Trp/Tyr/Phe) and flexible (Gly/Ser) residues. In addition, Fab$_{UNCL}$ contains several Pro residues in the CDR-H3 segment (Fig-
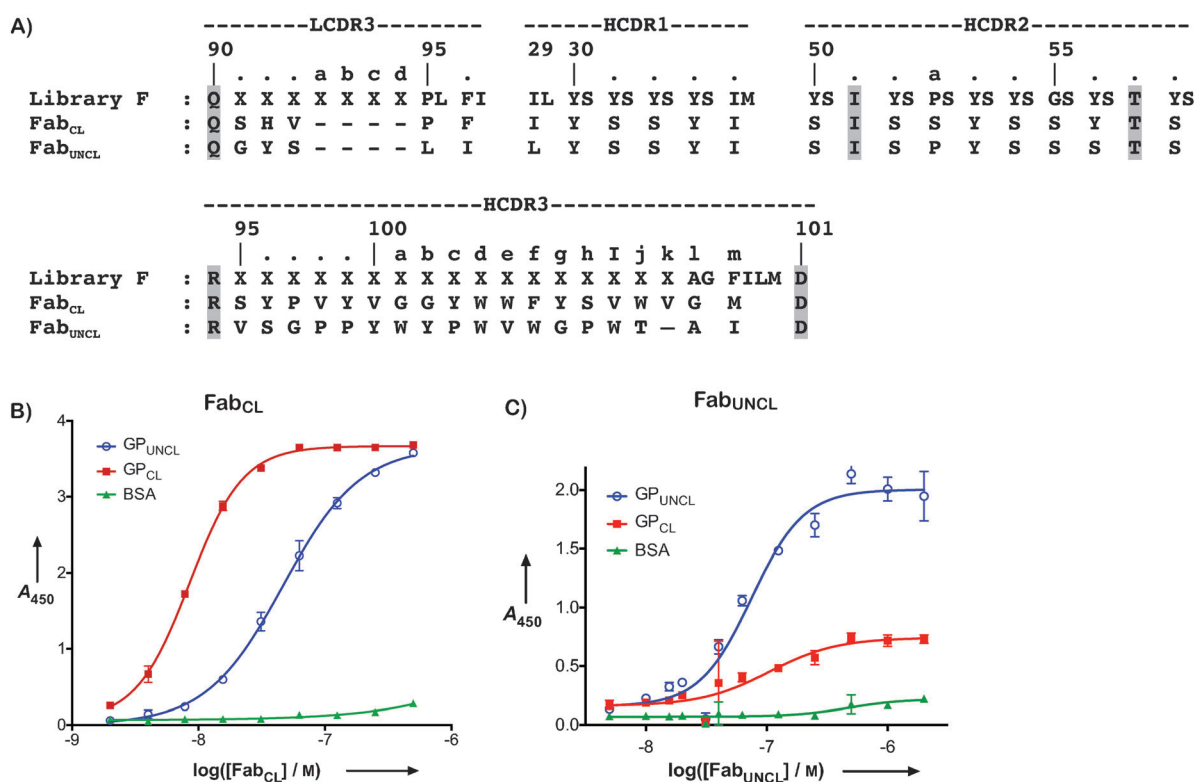

Figure 2. A) Amino acid sequences for Library F, Fab$_{CL}$, and Fab$_{UNCL}$. Invariant residues in Library F are highlighted in grey. Oligos of varying length were used during library construction in the LCDR3 (3–7 X residues) and HCDR3 (1–17 X residues) regions. X encodes nine residues, Tyr/Ser/Gly/Ala/Phe/Trp/His/Pro/Val, in a 5:4:4:2:1:1:1:1:1 ratio. B and C) ELISA binding profiles for B) Fab$_{CL}$ and C) Fab$_{UNCL}$ against GP$_{UNCL}$ and GP$_{CL}$. BSA was included as a negative control protein. The half-maximal binding titers (EC$_{50}$) were as follows: B) 1.7 nᴍ for Fab$_{CL}$ against GP$_{CL}$ and 13 nᴍ against GP$_{UNCL}$; C) 75 nᴍ for Fab$_{UNCL}$ against GP$_{UNCL}$.

These are not the final page numbers! ↗↗

ure 2 A). The length of the CDR-H3 regions suggests that this segment constitutes a major element of the structural paratope for both Fabs.

Binding and neutralization profiles

Fab_{CL} and Fab_{UNCL} proteins were expressed periplasmically in *E. coli* and purified. Binding profiles toward GP_{CL}, GP_{UNCL}, and BSA were assessed by ELISA (Figure 2 B and 2 C). Fab_{CL} demonstrated preferential binding to GP_{CL}, with a half-maximal binding titer (EC_{50}) of 1.7 nM, but also exhibited cross-reactivity with GP_{UNCL} (EC_{50} of 13 nM). No binding to BSA was observed. Fab_{UNCL} was specific for GP_{UNCL}, with an EC_{50} of 75 nM and only low levels of binding to GP_{CL}. Fab_{UNCL} showed no appreciable binding to BSA.

We used a vesicular stomatitis virus particle bearing EBOV GP in place of the native envelope glycoprotein (VSV-GP pseudotype) to determine whether these two antibodies had neutralization activity for GP-mediated viral entry. As with the purified ectodomain, the VSV-GP construct (VSV-GP_{UNCL}) lacks the mucin-like domain. Furthermore, the viral genome encodes the enhanced green fluorescent protein (eGFP), allowing quantification of infection by fluorescence microscopy. VSV-GP particles can be treated with thermolysin in situ to mimic the cleaved form, VSV-GP_{CL},[14, 16, 20] allowing antibody neutralization potential to be tested against viruses displaying both forms of GP. For these experiments, the IgG1 versions of both Fab_{CL} and Fab_{UNCL} (IgG_{CL} and IgG_{UNCL}) were produced in HEK293T cells and purified. IgG_{CL} had enhanced stability relative to Fab_{CL} and was therefore used for the neutralization studies. Fab_{UNCL} and IgG_{UNCL} behaved equally well; therefore, Fab_{UNCL} was used due to the higher yield. Vero cells were used as the infection host.

As shown in Figure 3 A, IgG_{CL} neutralized VSV-GP_{CL} in a dose-dependent manner with an IC_{50} of 87 nM. At the highest IgG_{CL} concentrations tested (670 nM), the maximum neutralization observed was approximately 75 %. Previous studies by Shedlock et al. identified a monkey antibody, JP3K11, that bound to and neutralized Cat L-cleaved GP, suggesting that epitopes on GP_{CL} could be targeted by antibodies.[44] Our results with IgG_{CL} confirm that epitopes on GP_{CL} can be targeted for virus neutralization. However, unlike JP3K11, which did not discriminate between viruses containing uncleaved and cleaved GP, IgG_{CL} showed no appreciable neutralization activity toward VSV-GP_{UNCL} at the highest antibody concentration tested (Figure 3 C). These results indicate that the neutralization epitope for IgG_{CL} is not exposed prior to endosomal uptake. Furthermore, the specific neutralization activity of IgG_{CL} toward the cleaved form of the glycoprotein matches the preferential binding of Fab_{CL} for GP_{CL} as observed by ELISA.

Fab_{UNCL} specifically neutralized VSV-GP_{UNCL} with an IC_{50} of 1 μM, and up to approximately 80 % neutralization at the highest Fab concentration (3.2 μM) (Figure 3 B). No neutralization of the VSV-GP_{CL} particle was observed, even at the highest Fab_{UNCL} concentration tested. Therefore, IgG_{CL} and Fab_{UNCL} have orthogonal neutralization profiles for the cleaved and prefusion forms of GP, respectively.
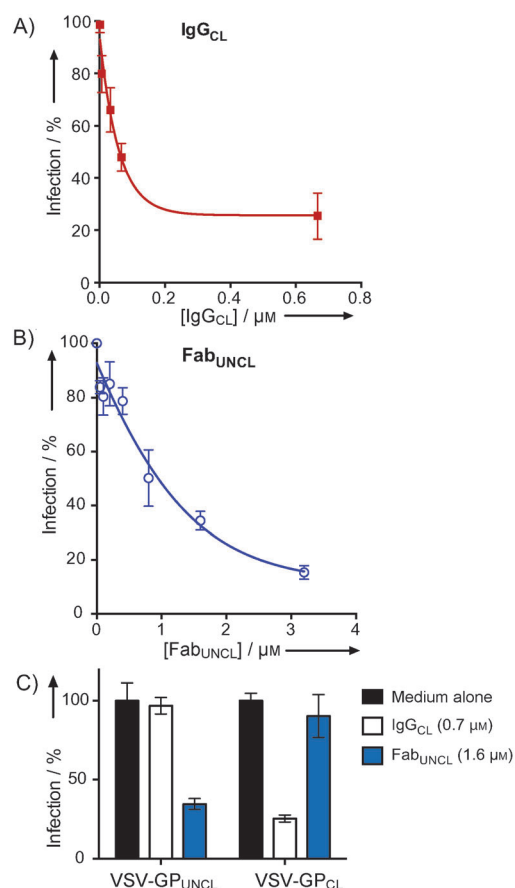

Figure 3. Neutralization profiles of Fab_{UNCL} and Fab_{CL} for infection of Vero cells. A) IgG_{CL} versus VSV-GP_{CL}. IgG_{CL} inhibits VSV-GP_{CL} in a dose-dependent manner, with an IC_{50} of 87 nM. B) Fab_{UNCL} versus VSV-GP_{UNCL}. Fab_{UNCL} inhibits VSV-GP_{UNCL} with an IC_{50} of 1 μM. C) Neutralization profiles of IgG_{CL} and Fab_{UNCL} against VSV-GP_{UNCL} and VSV-GP_{CL} at high antibody concentrations. Neutralization profiles of the two antibodies are completely orthogonal and match the recognition specificities determined by ELISA.

Competition ELISAs demonstrate that Fab_{CL} and Fab_{UNCL} bind novel epitopes

We next explored if the two synthetic antibodies bound to known structural epitopes on the prefusion or proteolytically cleaved forms of GP. Although the neutralization profiles of the two Fabs were specific, the moderate cross-reactivity of Fab_{CL} and Fab_{UNCL} for the different forms of GP (Figure 2 B) suggested that there might be some overlap in their structural epitopes. We therefore performed competition ELISAs to dissect recognition profiles. Fab_{CL} was biotinylated ($bFab_{CL}$), and binding to immobilized GP_{CL} (detected with a streptavidin/horseradish peroxidase conjugate) was quantified in the presence of four nonbiotinylated competitors: Fab_{CL} (positive control), Fab_{UNCL}, KZ52 IgG (an antibody isolated from an EBOV human survivor library[45]), and the soluble isolated form of the 248-residue luminal domain C of NPC1 (Loop C). Recently, it has been established that Loop C binds specifically and directly to GP_{CL}.[19] Furthermore, Loop C is able to inhibit the infection of VSV-GP_{CL}.[19] These results indicated that Loop C acts as an essential determinant for the recognition of NPC1 by cleaved GP within en-

⬉⬉ These are not the final page numbers!

dosomes. We included Loop C in the competition ELISA to see if Loop C would inhibit $bFab_{CL}$ binding since one potential mechanism for inhibition of $VSV-GP_{CL}$ entry would be direct competition for NPC1. We found that binding of Fab_{CL} was not reduced in the presence of Loop C, even at concentrations near 1 μM. Therefore, the Fab_{CL} binding epitope is distinct from that of Loop C. Additionally, neither Fab_{UNCL} nor KZ52 IgG reduced the binding of $bFab_{CL}$, indicating that Fab_{CL} binds a structural epitope distinct from those bound by Fab_{UNCL} and KZ52. As expected, Fab_{CL} (nonbiotinylated) reduced the binding of $bFab_{CL}$ in a concentration-dependent manner with an IC_{50} of 90 nM (Figure 4 A).

were found to bind similar regions at the base of the chalice in the prefusion forms of GP from the *Zaire* and *Sudan* species, respectively.[36, 37] We therefore sought to determine if Fab_{UNCL} bound *Zaire* GP_{UNCL} at a similar location as did KZ52. Again, as expected, Fab_{UNCL} (nonbiotinylated) was able to compete with $bFab_{UNCL}$, with an IC_{50} of 200 nM. However, neither KZ52 IgG nor Fab_{CL} were able to reduce binding of $bFab_{UNCL}$, indicating that neither KZ52 nor Fab_{CL} have overlapping structural epitopes with Fab_{UNCL}.

pH-dependent recognition properties of Fab_{UNCL} and Fab_{CL}

Following initial cell surface-binding events, EBOV is taken up into the endosome via macropinocytosis, where GP proteolytic cleavage and GP-mediated viral membrane fusion occurs.[46, 47] It is believed that antibodies targeting prefusion GP (e.g., KZ52 and 16F6) function by stabilizing the prefusion conformation and preventing transformations (conformational or other) that are required for membrane fusion.[37] It therefore follows that such neutralizing antibodies must retain binding activity under the acidic conditions of the endosome for a long enough period of time to sequester GP. Presumably, neutralizing antibodies targeting other viruses that enter through the endosome and prevent membrane fusion must also have the capacity to function under endosomal conditions. For example, it has been reported that an antibody that targets the envelope protein of West Nile Virus (E16) is colocalized to the endosomal compartments along with the virus during entry.[48] Therefore, the likely mechanism of E16 action is to inhibit acid-dependent fusion-associated conformational changes. Endosomal pH is thought to be required for GP-mediated entry for several reasons. First, most endosomal cysteine proteases have optimal activity at pH~5, and their activity is critical for generation of the proteolytic intermediate.[13] Second, pH-dependent conformational transitions result in activation of the GP2 fusion loop.[14b] Third, folding of the GP2 six-helix bundle that provides the driving force for membrane fusion is more stable under acidic conditions.[49, 50]

Treatment of $VSV-GP_{UNCL}$ with thermolysin primes GP for fusion by mimicking endosomal proteolytic cleavage; therefore, $VSV-GP_{CL}$ can bypass the requirement for cathepsin cleavage within endosomes.[14] However, the entry of $VSV-GP_{CL}$ as well as $VSV-GP_{UNCL}$ likely occurs in the endosome and not at the cell surface.[16–19, 46] We therefore explored the recognition profiles of Fab_{CL} and Fab_{UNCL} at pH 4.5 (the pH of the late endosome/lysosome) to gain insight into the stability of the Fab–GP complexes under conditions that mimic those found in the endocytic pathway (Figure 5). It was recently reported that the binding of KZ52 to *Zaire* EBOV GP_{CL} was not affected at endosomal pH, suggesting that KZ52 remains bound to GP in the endosome.[16] These data thus support an endosomal mode of action for KZ52.[16] We found that Fab_{CL} retained affinity for GP_{CL} at pH 4.5 ($EC_{50} = 10$ nM). Interestingly, under these conditions, the specificity of Fab_{CL} for GP_{CL} over GP_{UNCL} was markedly attenuated relative to pH 7.5 (at pH 4.5, EC_{50} for GP_{CL} was less than twofold lower than GP_{UNCL}). One possible explanation for this result is that GP_{UNCL} undergoes a subtle conformational
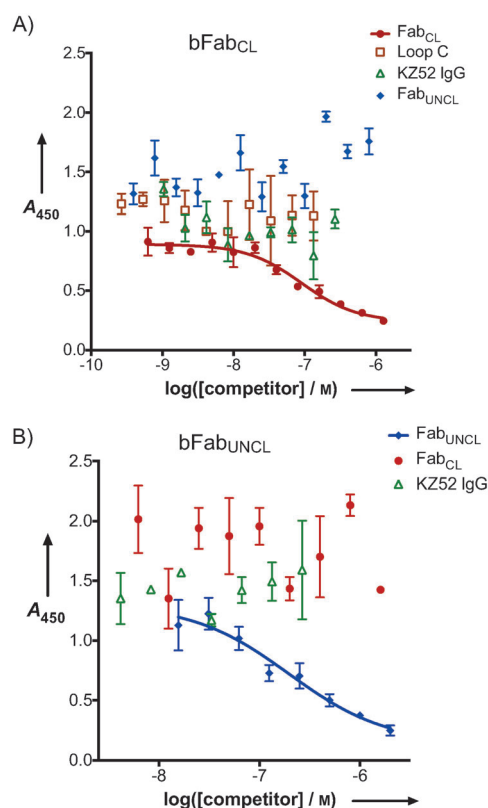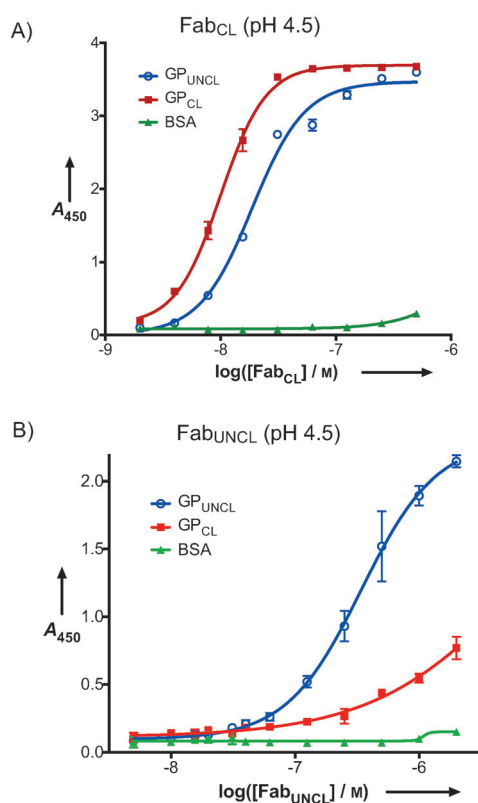
Figure 4. Competition ELISAs. A) Biotinylated Fab_{CL} ($bFab_{CL}$) versus four unbiotinylated competitors: Fab_{CL}, Fab_{UNCL}, KZ52, and the luminal domain C of the endosomal cholesterol transporter NPC1 (Loop C).[19] Fab_{CL} competes with $bFab_{CL}$; data were fit to a four-parameter logistic equation, yielding an IC_{50} of 90 nM. None of the other proteins reduced the binding of $bFab_{CL}$ and therefore, the data were not fit to an equation in these cases. B) Biotinylated Fab_{UNCL} ($bFab_{UNCL}$) versus three unbiotinylated competitors: Fab_{UNCL}, Fab_{CL}, and KZ52 IgG. Neither Fab_{CL} nor KZ52 IgG had an effect on $bFab_{UNCL}$ binding. Fab_{UNCL} competed with $bFab_{UNCL}$ with an IC_{50} of 200 nM.

Similar experiments were performed with $bFab_{UNCL}$ against GP_{UNCL}, although Loop C was not included in this competition because Loop C does not bind GP_{UNCL}.[19] GP_{UNCL} is heavily glycosylated within the mucin-like domain and glycan cap, though all constructs investigated here were performed with GP lacking the mucin-like domain. A "hotspot" for neutralization was recently described: the structural epitopes for KZ52 and 16F6, a murine antibody isolated from vaccinated mice,

These are not the final page numbers! ↗↗

A)

Fab$_{CL}$ (pH 4.5)

B)

Fab$_{UNCL}$ (pH 4.5)

Figure 5. Fab binding to GP$_{UNCL}$ and GP$_{CL}$ at pH 4.5. BSA was included as a control. The half-maximal binding titers were: A) 10 nM for Fab$_{CL}$ against GP$_{CL}$ and 18 nM against GP$_{UNCL}$; B) 340 nM for Fab$_{UNCL}$ against GP$_{UNCL}$.

change upon exposure to low pH, which can be detected by an increase in Fab$_{CL}$ binding. However, we cannot rule out the possibility that pH-induced structural effects on the Fab$_{CL}$ CDR segments are responsible for this pH-dependent recognition profile. pH-dependent conformational changes have been reported in full-length IgGs and Fab fragments, but these generally occur in conditions below pH 3.5.[51, 52] Therefore, we believe it is less likely that Fab conformational changes are responsible for the change in recognition profiles observed here (pH 4.5). In contrast to Fab$_{CL}$, Fab$_{UNCL}$ retained its selectivity for GP$_{UNCL}$ over GP$_{CL}$ at pH 4.5, but had a lower overall affinity for GP$_{UNCL}$ (EC$_{50}$ = 340 nM). Again, these results raise the possibility that there are some conformational differences in GP$_{UNCL}$ at neutral versus endosomal pH that are detected upon binding of Fab$_{UNCL}$. Neither Fab$_{CL}$ nor Fab$_{UNCL}$ had any appreciable affinity for BSA under these conditions.

Conclusions

We describe the isolation and characterization of two synthetic antibodies (Fab$_{CL}$/IgG$_{CL}$ and Fab$_{UNCL}$) that have distinct recognition and neutralization properties for mimics of the prefusion and proteolytically cleaved forms of EBOV GP. Several antibodies have been described against the prefusion form of GP, but the two that have been characterized structurally (KZ52 and 16F6) bind to a localized position at the base of the GP trimer.[36, 37] We found that Fab$_{UNCL}$ likely binds a novel epitope

on GP$_{UNCL}$, as it does not compete for binding with KZ52 IgG. Additionally, Fab$_{CL}$/IgG$_{CL}$ binds a novel epitope on GP$_{CL}$. While some cross-reactivity for GP$_{CL}$ and GP$_{UNCL}$ was observed for Fab$_{CL}$ binding, IgG$_{CL}$ had a very distinct specificity for the neutralization of VSV-GP$_{CL}$. Interestingly, although the ability of Fab$_{CL}$ to bind GP$_{CL}$ was retained at low pH, its ability to distinguish GP$_{CL}$ from GP$_{UNCL}$ was diminished relative to pH 7.5. Therefore, the likely mechanism of specificity for neutralization of GP$_{CL}$ involves preferential binding at pH 7.5, prior to VSV-GP$_{CL}$ uptake. These results confirm that epitopes on GP$_{CL}$ are available for neutralization, although such epitopes may be exposed only within the endosome. Additionally, the differences in binding of Fab$_{CL}$ and Fab$_{UNCL}$ to GP$_{UNCL}$ at low pH raises the possibility that GP$_{UNCL}$ undergoes a subtle conformational change upon exposure to low pH, perhaps facilitating proteolytic cleavage.

A growing body of work has demonstrated the utility of synthetic antibody and fragment repertoires for identification of antibodies for therapeutic or research purposes.[38, 40–42, 53] Here, we have expanded the scope to include targeting of suspected structural intermediates in viral entry into host cells. In the specific case of EBOV, these results provide access to novel reagents for the dissection of the viral entry and membrane fusion pathways. Furthermore, this work suggests that future immunotherapeutic development could center around novel epitopes on GP$_{UNCL}$ and GP$_{CL}$.

Experimental Section

Antibody selection on phage: GP$_{UNCL}$ and GP$_{CL}$ ectodomains were expressed and processed as described previously.[16] Biopanning, direct phage ELISAs, and single-point competitive phage ELISAs were performed as described previously.[39] Briefly, in sorting for GP$_{CL}$ specific Fabs, phage pools representing a phage-displayed synthetic antibody library (Library F) were cycled through five rounds of binding selection with GP$_{CL}$ immobilized on 96-well Maxisorp immunoplates (Fisher Scientific, Nepean, ON, Canada) as the capture target. Stringency was increased in the panning process by 1) preincubation of the phage pool in immunoplates coated with GP$_{UNCL}$ (5 µg mL^{-1}) for 1 h at room temperature before the phage pool was transferred to GP$_{CL}$-immobilized immunoplates for rounds 2–5, and 2) decreasing the antigen concentration used for coating the immunoplates from 5 µg mL^{-1} for rounds 2 and 3 to 2 µg mL^{-1} for rounds 4 and 5. The same strategy was also applied for the selection against GP$_{UNCL}$, except that only four rounds of selection were performed. After selection, 96 clones each from rounds 4 and 5 of the GP$_{CL}$ selection and 96 clones from round 4 of the GP$_{UNCL}$ selection were grown overnight in 96-well deep well plates with 2YT broth supplemented with carbenicillin and M13K07. The culture supernatants were used directly in phage ELISAs to identify binding clones specifically targeting GP$_{CL}$ over GP$_{UNCL}$ or vice versa. Clones exhibiting phage ELISA signals at least tenfold higher than those of the control (BSA) and at least twofold higher than those of the other form of GP were subjected to DNA sequence analysis.

Fab protein expression: The phage display vectors were converted to Fab protein expression vectors by insertion of a stop codon and a His$_6$ tag upstream of the P3 gene fusion. Fab proteins were expressed periplasmically in *E. coli* BL21(DE3) (Invitrogen) by

growth in low-phosphate media at 30 °C for 18–22 h. The cells were harvested by centrifugation and lysed by using the "Bug Buster" reagent according to the manufacturer's instructions (Novagen, Madison, WI). The lysate was subjected to centrifugation, and the supernatant was applied to a nickel column (Ni-NTA resin, Qiagen, Valencia, CA). The column was washed twice, first with 20 mM imidazole and then with 50 mM imidazole. The protein was eluted with 500 mM imidazole. The eluent was dialyzed into phosphate-buffered saline (PBS), pH 7.4 and applied to a protein A affinity column (beads from Pierce Thermo Scientific, Rockford, IL) to remove unpaired heavy or light chains. The beads were washed with PBS, pH 8.0 (2–4 column volumes), and the Fab proteins were eluted with 100 mM glycine, pH 2.0. The eluted Fab proteins were immediately neutralized to ~pH 7.4 using 1 M Tris, pH 8.0. Fractions containing the Fab proteins were dialyzed overnight into PBS, pH 7.4 and were used directly in binding or neutralization assays, or flash-frozen and stored at −80 °C for later use. The Fab protein concentration was determined by measuring the absorbance at 280 nm.

IgG protein expression: DNA for the variable domains were subcloned into pMAZ-IgL and pMAZ-IgH vectors for expression of full-length IgG1 molecules.[55] Vectors for the heavy chain and light chain were transfected into HEK293F cells using the Freestyle Max transfection reagent (Invitrogen), according to the manufacturer's instructions. Cell cultures were incubated at 37 °C for 5–7 days post-transfection. After incubation, the cultures were centrifuged, and the supernatant was applied to a protein A affinity column (Pierce, Thermo Scientific, Rockford, IL). The eluent was dialyzed into PBS, pH 7.4 overnight, and the IgG protein was concentrated and used directly in neutralization assays.

Binding ELISAs: Target proteins were directly immobilized on 96-well Maxisorp plates (Corning Incorporated, Corning, NY; $GP_{UNCL} = 0.4$ μg per well; $GP_{CL} = 0.25$ μg per well) by incubation in $NaHCO_3$, pH 8.0 at room temperature for 1 h. Phosphate-buffered saline (PBS, pH 7.4) containing 3% BSA was used to block the wells after target immobilization (incubation for 45 min at room temperature). The Fabs were diluted into PBS containing 0.05% (*v/v*) Tween20 (PBS-T), pH 7.4, applied to the wells, and incubated at room temperature for 1 h. The plates were washed with PBS-T and incubated for 45 min with horseradish peroxidase/anti-His$_6$ antibody conjugate (1:3000 dilution in PBS-T). The wells were washed with PBS-T, developed with 3,3′,5,5′-tetramethylbenzidine (TMB) substrate, and quenched with 1.0 M H_2SO_4. The absorbance at 450 nm was determined. The data were fit to a standard four-parameter logistic equation by using GraphPad Prism (GraphPad Software, La Jolla, CA). The half-maximal binding (EC_{50}) values were obtained from the inflection point of the curve.

Similar experiments were conducted at pH 4.5. In these experiments, the pH of the PBS-T buffer used for dilution of the Fabs was pH 4.5. The rest of the ELISA was conducted as described above.

Virus neutralization assay: For the virus neutralization assay, we used a vesicular stomatitis virus that is pseudotyped to display EBOV GP on its surface in place of its native glycoprotein (VSV-GP). The viral genome encodes the enhanced green fluorescent protein (eGFP); therefore, infection can be scored by counting fluorescent cells after infection. VSV-GP was made in 293T cells as has been described previously.[14, 56] Briefly, the virus-containing supernatants were harvested and concentrated by pelleting through a 10% sucrose cushion. Virus stocks were titered by infecting Vero (African green monkey kidney) cells with serial dilutions and counting GFP-

positive cells by fluorescence microscopy. Typical titers for VSV-GP were 10^9 infectious units (IU) per mL. Aliquots were stored at −80 °C in 10% sucrose. VSV-GP was used to infect Vero cells at approximate multiplicities of infection (MOIs) of 0.1 to 1.0 in Dulbecco's modified Eagle medium (DMEM) containing 5% fetal bovine serum, such that 20–200 cells were infected per well. VSV-GP was either used directly in neutralization experiments (VSV-GP_{UNCL}) or pre-treated with thermolysin in situ, resulting in pseudotyped virus displaying GP_{CL} (VSV-GP_{CL}). To generate VSV-GP_{CL}, VSV-GP was treated with thermolysin (200 μg mL^{-1}, Sigma) in NT buffer (10 mM Tris·Cl, 135 mM NaCl) at pH 7.5 for 1 h at 37 °C. The reactions were neutralized with phosphoramidon (1 mM, Peptide International, Louisville, KY) and incubated on ice for at least 15 min before use. Vero cell monolayers (~7.5e^4 cells per well in a 48-well plate) were exposed to pseudotyped virus that had been preincubated with dilutions of Fab$_{UNCL}$ or IgG$_{CL}$. Infection was scored by manually counting eGFP-positive cells under a fluorescence microscope at 14–18 h postinfection.

Competition ELISAs: Fab$_{UNCL}$ and Fab$_{CL}$ proteins were biotinylated (bFab$_{UNCL}$ and bFab$_{CL}$, respectively) using a NHS-PEG4-biotin labeling kit (Thermo Scientific, Rockford, IL) according to the manufacturer's instructions. GP_{UNCL} or GP_{CL} were immobilized on 96-well Maxisorp plates (Corning Incorporated, Corning, NY) at concentrations of 0.4 μg per well or 0.25 μg per well, respectively. For Fab$_{UNCL}$ competition ELISAs, bFab$_{UNCL}$ was diluted to 6 μg mL^{-1} in PBS-T buffer in the absence and presence of varying amounts of three unbiotinylated competitors: Fab$_{UNCL}$, Fab$_{CL}$, and KZ52 IgG. For Fab$_{CL}$ competition ELISAs, bFab$_{CL}$ was diluted to 6 μg mL^{-1} in PBS-T buffer in the absence and presence of varying amounts of four unbiotinylated competitors: Fab$_{CL}$, Fab$_{UNCL}$, KZ52 IgG, and Loop C.[19] Mixtures of bFab$_{UNCL}$ or bFab$_{CL}$ ± competitors were applied to the wells and incubated at room temperature for 1 h. The plates were washed with PBS-T, then horseradish peroxidase/strepavidin conjugate (1:1000 dilution in PBS-T buffer) was added, and the plates were incubated for 45 min. The plates were then washed with PBS-T, developed with TMB substrate, and quenched with 1.0 M H_2SO_4. Absorbance at 450 nm was measured. For the dose–response curves, the data was fit to a standard four-parameter logistic equation using GraphPad Prism (GraphPad Software, La Jolla, CA). Half-maximal binding (EC_{50}) values were obtained from the inflection point of the curve.

Acknowledgements

These are not the final page numbers! ↗↗

[1] H. Feldmann, T. W. Geisbert, *Lancet* **2011**, *377*, 849–862.

[2] J. H. Kuhn, S. Becker, H. Ebihara, T. W. Geisbert, K. M. Johnson, Y. Kawaoka, W. I. Lipkin, A. I. Negredo, S. V. Netesov, S. T. Nichol, G. Palacios, C. J. Peters, A. Tenorio, V. E. Volchkov, P. B. Jahrling, *Arch. Virol.* **2010**, *155*, 2083–2103.

[3] N. Sullivan, Z. Y. Yang, G. J. Nabel, *J. Virol.* **2003**, *77*, 9733–9737.

[4] A. L. Hartman, J. S. Towner, S. T. Nichol, *Clin. Lab. Med.* **2010**, *30*, 161–177.

[5] J. F. Wamala, L. Lukwago, M. Malimbo, P. Nguku, Z. Yoti, M. Musenero, J. Amone, W. Mbabazi, M. Nanyunja, S. Zaramba, A. Opio, J. J. Lutwama, A. O. Talisuna, S. I. Okware, *Emerging Infect. Dis.* **2010**, *16*, 1087–1092.

[6] http://www.cdc.gov/ncidod/dvrd/spb/outbreaks/.

[7] S. C. Harrison, *Nat. Struct. Mol. Biol.* **2008**, *15*, 690–698.

[8] J. M. White, S. E. Delos, M. Brecher, K. Schornberg, *Crit. Rev. Biochem. Mol. Biol.* **2008**, *43*, 189–219.

[9] D. M. Eckert, P. S. Kim, *Annu. Rev. Biochem*. **2001**, *70*, 777–810.

[10] J. E. Lee, M. L. Fusco, A. J. Hessell, W. B. Oswald, D. R. Burton, E. O. Saphire, *Nature* **2008**, *454*, 177–182.

[11] J. E. Lee, E. O. Saphire, *Future Virol.* **2009**, *4*, 621–635.

[12] M. Brecher, K. L. Schornberg, S. E. Delos, M. L. Fusco, E. O. Saphire, J. M. White, *J. Virol.* **2012**, *86*, 364–372.

[13] K. Chandran, N. J. Sullivan, U. Felbor, S. P. Whelan, J. M. Cunningham, *Science* **2005**, *308*, 1643–1645.

[14] a) K. Schornberg, S. Matsuyama, K. Kabsch, S. E. Delos, A. Bouton, J. M. White, *J. Virol.* **2006**, *80*, 4174–4178; b) S. M. Gregory, E. Harada, B. Liang, S. E. Delos, J. M. White, L. K. Tamm, *Proc. Natl. Acad. Sci. USA* **2011**, *108*, 11211–11216.

[15] J. Misasi, K. Chandran, J. Y. Yang, B. Considine, N. J. Sullivan, C. M. Filone, L. E. Hensley, J. Cunningham, *J. Virol.* **2012**, *86*, 3284–3292.

[16] S. Bale, T. Liu, S. Li, Y. Wang, D. Abelson, M. Fusco, V. L. Woods, Jr., E. O. Saphire, *PLoS Neglected Trop. Dis.* **2011**, *5*, e1395.

[17] J. E. Carette, M. Raaben, A. C. Wong, A. S. Herbert, G. Obernosterer, N. Mulherkar, A. I. Kuehne, P. J. Kranzusch, A. M. Griffin, G. Ruthel, P. Dal Cin, J. M. Dye, S. P. Whelan, K. Chandran, T. R. Brummelkamp, *Nature* **2011**, *477*, 340–343.

[18] M. Côté, J. Misasi, T. Ren, A. Bruchez, K. Lee, C. M. Filone, L. Hensley, Q. Li, D. Ory, K. Chandran, J. Cunningham, *Nature* **2011**, *477*, 344–348.

[19] E. H. Miller, G. Obernosterer, M. Raaben, A. S. Herbert, M. S. Deffieu, A. Krishnan, E. Ndungo, R. G. Sandesara, J. E. Carette, A. I. Kuehne, G. Ruthel, S. R. Pfeffer, J. M. Dye, S. P. Whelan, T. R. Brummelkamp, K. Chandran, *EMBO J.* **2012**, *31*, 1947–1960.

[20] A. C. Wong, R. G. Sandesara, N. Mulherkar, S. P. Whelan, K. Chandran, *J. Virol.* **2010**, *84*, 163–175.

[21] D. R. Burton, J. Pyarti, R. Koduri, S. J. Sharp, G. B. Thornton, P. W. H. I. Parren, L. S. W. Sawyer, R. M. Hendry, N. Dunlop, P. L. Nara, M. Lamacchia, E. Garratty, E. R. Stiehm, Y. J. Bryson, Y. Cao, J. P. Moore, D. D. Ho, C. F. Barbas, III., *Science* **1994**, *266*, 1024–1027.

[22] R. Pantophlet, I. A. Wilson, D. R. Burton, *Protein Eng. Des. Sel.* **2004**, *17*, 749–758.

[23] R. Pantophlet, E. O. Saphire, P. Poignard, P. W. Parren, I. A. Wilson, D. R. Burton, *J. Virol.* **2003**, *77*, 642–658.

[24] A. Mor, E. Segal, B. Mester, B. Arshava, O. Rosen, F. X. Ding, J. Russo, A. Dafni, F. Schvartzman, T. Scherf, F. Naider, J. Anglister, *Biochemistry* **2009**, *48*, 3288–3303.

[25] D. C. Ekiert, G. Bhabha, M. A. Elsliger, R. H. E. Friesen, M. Jongeneelen, M. Throsby, J. Goudsmit, I. A. Wilson, *Science* **2009**, *324*, 246–251.

[26] D. C. Ekiert, R. H. E. Friesen, G. Bhabha, T. Kwaks, M. Jongeneelen, W. Yu, C. Ophorst, F. Cox, H. J. W. M. Korse, B. Brandenburg, R. Vogels, J. P. J. Brakenhoff, R. Kompier, M. H. Koldijk, M. H. Cornelissen, L. A. H. M. Poon, L. L. M. M. Peiris, W. Koudstaal, I. A. Wilson, I. A. J. Goudsmit, *Science* **2011**, *333*, 843–850.

[27] D. Corti, J. Voss, S. J. Gamblin, G. Codoni, A. Macagno, D. Jarrossay, S. G. Vachieri, D. Pinna, A. Minola, F. Vanzetta, C. Silacci, B. M. Fernandez-Rodriguez, G. Agatic, S. Bianchi, I. Giacchetto-Sasselli, L. Calder, F. Sallusto, P. Collins, L. F. Haire, N, Temperton, J. P. M. Langedijk, J. J. Skehel, A. Lanzavecchia, *Science* **2011**, *333*, 850–856.

[28] D. R. Burton, C. F. Barbas, M. A. Persson, S. Koenig, R. M. Chanock, R. A. Lerner, *Proc. Natl. Acad. Sci. USA* **1991**, *88*, 10134–10137.

[29] A. K. Kashyap, J. Steel, A. F. Oner, M. A. Dillon, R. E. Swale, K. M. Wall, K. J. Perry, A. Faynboym, M. Ilhan, M. Horowitz, L. Horowitz, P. Palese, R. R. Bhatt, R. A. Lerner, *Proc. Natl. Acad. Sci. USA* **2008**, *105*, 5986–5991.

[30] X. Wu, Z. Y. Yang, Y. Li, C. M. Hogerkorp, W. R. Schief, M. S. Seaman, T. Zhou, S. D. Schmidt, L. Wu, L. Xu, N. S. Longo, K. McKee, S. O'Dell, M. K. Louder, D. L. Wycuff, Y. Feng, M. Nason, N. Doria-Rose, M. Connors, P. D. Kwong, M. Roederer, R. T. Wyatt, G. J. Nabel, J. R. Mascola, *Science* **2010**, *329*, 856–861.

[31] G. Stiegler, R. Kunert, M. Purtscher, S. Wolbank, R. Voglauer, F. Steindl, H. Katinger, *AIDS Res. Hum. Retroviruses* **2001**, *17*, 1757–1765.

[32] T. G. Ksiazek, P. E. Rollin, A. J. Williams, D. S. Bressler, M. L. Martin, R. Swanepoel, F. J. Burt, P. A. Leman, A. S. Khan, A. K. Rowe, R. Mukunu, A. Sanchez, C. J. Peters, *J. Infect. Dis.* **1999**, *179*, S177–S187.

[33] O. Dolnik, V. Volchkova, W. Garten, C. Carbonnelle, S. Becker, J. Kahnt, U. Ströher, H. D. Klenk, V. Volchkov, *EMBO J.* **2004**, *23*, 2175–2184.

[34] J. R. Francica, A. Varela-Rohena, A. Medvec, G. Plesa, J. L. Riley, P. Bates, *PLoS Pathog.* **2010**, *6*, e1001098.

[35] T. Maruyama, L. L. Rodriguez, P. B. Jahrling, A. Sanchez, A. S. Khan, S. T. Nichol, C. J. Peters, P. W. Parren, D. R. Burton, *J. Virol.* **1999**, *73*, 6024–6030.

[36] J. M. Dias, A. I. Kuehne, D. M. Abelson, S. Bale, A. C. Wong, P. Halfmann, M. A. Muhammad, M. L. Fusco, S. E. Zak, E. Kang, Y. Kawaoka, K. Chandran, J. M. Dye, E. O. Saphire, *Nat. Struct. Mol. Biol.* **2011**, *18*, 1424–1427.

[37] J. E. Lee, E. O. Saphire, *Curr. Opin. Struct. Biol.* **2009**, *19*, 408–417.

[38] S. Koide, S. S. Sidhu, *ACS Chem. Biol.* **2009**, *4*, 325–334.

[39] F. A. Fellouse, K. Esaki, S. Birtalan, D. Raptis, V. J. Cancasci, A. Koide, P. Jhurani, M. Vasser, C. Wiesmann, A. A. Kossiakoff, S. Koide, S. S. Sidhu, *J. Mol. Biol.* **2007**, *373*, 924–940.

[40] J. Gao, S. S. Sidhu, J. A. Wells, *Proc. Natl. Acad. Sci. USA* **2009**, *106*, 3071–3076.

[41] J. D. Ye, V. Tereshko, J. K. Frederiksen, A. Koide, F. A. Fellouse, S. S. Sidhu, S. Koide, A. A. Kossiakoff, J. A. Piccirilli, *Proc. Natl. Acad. Sci. USA* **2008**, *105*, 82–87.

[42] Y. Koldobskaya, E. M. Duguid, D. M. Schechner, N. B. Suslov, J. Ye, S. S. Sidhu, D. P. Bartel, S. Koide, A. A. Kossiakoff, J. A. Piccirilli, *Nat. Struct. Mol. Biol.* **2011**, *18*, 100–106.

[43] D. Dube, M. B. Brecher, S. E. Delos, S. C. Rose, E. W. Park, K. L. Schornberg, J. H. Kuhn, J. M. White, *J. Virol.* **2009**, *83*, 2883–2891.

[44] D. J. Shedlock, M. A. Bailey, P. M. Popernack, J. M. Cunningham, D. R. Burton, N. J. Sullivan, *Virology* **2010**, *401*, 228–235.

[45] T. Maruyama, L. L. Rodriguez, P. B. Jahrling, A. Sanchez, A. S. Khan, S. T. Nichol, C. J. Peters, P. W. H. I. Parren, D. R. Burton, *J. Virol.* **1999**, *73*, 6024–6030.

[46] M. F. Saeed, A. A. Kolokoltsov, T. Albrecht, R. A. Davey, *PLoS Pathog.* **2010**, *6*, e1001110.

[47] N. Mulherkar, M. Raaben, J. C. de La Torre, S. P. Whelan, K. Chandran, *Virology* **2011**, *419*, 72–83.

[48] B. S. Thompson, B. Moesker, J. M. Smit, J. Wilschut, M. S. Diamond, D. H. Fremont, *PLoS Pathog.* **2009**, *5*, e1000453.

[49] J. S. Harrison, C. D. Higgins, K. Chandran, J. R. Lai, *Protein Sci.* **2011**, *20*, 1587–1596.

[50] J. S. Harrison, J. F. Koellhoffer, K. Chandran, J. R. Lai, *Biochemistry* **2012**, *51*, 2515–2525.

[51] K. Welfle, R. Misselwitz, G. Hausdorf, W. Hohne, H. Welfle, *Biochim. Biophys. Acta Protein Struct. Mol. Enzymol.* **1999**, *1431*, 120–131.

[52] J. Buchner, R. Rudolph, H. Lilie, *J. Mol. Biol.* **2002**, *318*, 829–836.

[53] J. Wojcik, O. Hantschel, F. Grebien, I. Kaupe, K. L. Bennett, J. Barkinge, R. B. Jones, A. Koide, G. Superti-Furga, S. Koide, *Nat. Struct. Mol. Biol.* **2010**, *17*, 519–527.

[54] W. Weissenhorn, A. Carfi, K. H. Lee, J. J. Skehel, D. C. Wiley, *Mol. Cell* **1998**, *2*, 605–616.

[55] Y. Mazor, I. Barnea, I. Keydar, I. Benhar, *J. Immunol. Methods* **2007**, *321*, 41–59.

[56] A. Takada, C. Robison, H. Goto, A. Sanchez, K. G. Murti, M. A. Whitt, Y. Kawaoka, *Proc. Natl. Acad. Sci. USA* **1997**, *94*, 14764–14769.

[57] a) H. Karauzum, G. Chen, L. Abaandou, M. Mahmoudieh, A. R. Boroun, S. Shulenin, V. S. Devi, E. Stavale, K. L. Warfield, L. Zeitlin, C. J. Roy, S. S. Sidhu, M. J. Aman, *J. Biol. Chem.* **2012**, *287*, 25203–25215; b) J. D. Laver,

↖↖ **These are not the final page numbers!**

K. Ancevicius, P. Sollazzo, J. T. Westwood, S. S. Sidhu, H. D. Lipshitz, C. A. Smibert, *Mol. Biosyst.* **2012**, *8*, 1650–1657; c) K. Colwill, Renewable Protein Binder Working Group, S. Graslund, *Nat. Methods* **2011**, *8*, 551–558; d) O. Qazi, M. Rani, A. J. Gnanam, T. W. Cullen, C. M. Stead, H. Kensing, K. McCaul, S. Ngugi, J. L. Prior, A. Lipka, J. M. Nagy, C. W. Gregory, B. M. Judy, S. V. Harding, R. W. Titball, S. S. Sidhu, M. S. Trent, G. B. Kitto, A. Torres, D. M. Estes, B. Iverson, G. Georgiou, K. A. Brown, *Faraday Discuss.* **2011**, *149*, 23–36.

These are not the final page numbers! ↗↗
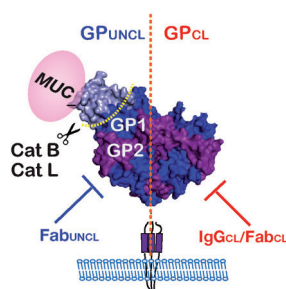
FULL PAPERS

J. F. Koellhoffer, G. Chen, R. G. Sandesara,
S. Bale, E. Ollmann Saphire,
K. Chandran,* S. S. Sidhu,* J. R. Lai*

■■ – ■■

Two Synthetic Antibodies that Recognize and Neutralize Distinct Proteolytic Forms of the Ebola Virus Envelope Glycoprotein

A tale of two antibodies: Ebola virus (EBOV) causes severe hemorrhagic fever associated with high mortality rates. Here we report the identification of two synthetic antibody fragments that have orthogonal binding and neutralization profiles against two prefusion forms of the EBOV glycoprotein. These antibodies provide new tools for dissecting intermediates of viral membrane fusion and entry. (56 words)

↖↖ These are not the final page numbers!